Experimental Mechanics (2021) 61:253–261
https://doi.org/10.1007/s11340-020-00667-5

SP ISS: EXPERIMENTAL ADVANCES IN CARDIOVASCULAR BIOMECHANICS

MicroCT Imaging of Heart Valve Tissue in Fluid

S.E. Stephens[1] · M. Bean[1] · H. Surber[1] · N.B. Ingels[1] · H.K. Jensen[1,2] · S. Liachenko[3] · J.F. Wenk[4] · M.O. Jensen[1]

Received: 4 February 2020 / Revised: 12 August 2020 / Accepted: 22 September 2020 / Published online: 27 October 2020
© Society for Experimental Mechanics 2020

Abstract

Background Heart valve computational models require high quality geometric input data, commonly obtained using micro-computed tomography. Whether in the open or closed configuration, most studies utilize dry valves, which poses significant challenges including gravitational and surface tension effects along with desiccation induced mechanical changes.

Objective These challenges are overcome by scanning in a stress-free configuration in fluid. Utilizing fluid backgrounds however reduces overall contrast due to the similar density of fluid and tissue.

Methods The work presented here demonstrates imaging of the mitral valve by utilizing an iodine-based staining solution to improve the contrast of valve tissue against a fluid background and investigates the role of stain time and concentration.

Results It is determined that an *Olea europaea* oil bath with a relatively high concentration, short stain time approach produces high quality imagery suitable for creating accurate 3D renderings.

Conclusions Micro-CT scanning of heart valves in fluid is shown to be feasible using iodine staining techniques.

Keywords MicroCT · μCT · Contrast-enhanced · Mitral valve

Introduction

High resolution in vitro imaging of the mitral valve (MV) has been successfully demonstrated using several imaging modalities such as high Tesla MRI [1] and micro-computed tomography (μCT) [2–4]. Challenges remain to image the valve in its stress free, natural state submerged in a liquid fluid. We reported for the first time the use of 7 T MRI to obtain images of the valve in its natural state submerged and neutrally buoyant in a liquid fluid [1]. However, using high resolution MRI presents several challenges, such as time of scanning, cost, type of fluid, materials restrictions, etc.

Of critical importance to the utility of 3D MV datasets for use in computational simulations is the shape of the annulus and position/orientation of the papillary muscles (PM) [5]. The geometric configuration of the valve, including annulus shape [6, 7] and PM position and orientation [8, 9], directly affects the strain distribution and coaptation, altering valve competence. As MV 3D datasets are frequently used as input for Finite Element Analysis (FEA) and Computational Fluid Dynamics (CFD) studies, the physiological realism of the scanned geometry should be as high as possible to ensure reliable simulation results. Prior work by our group has demonstrated the use of an imaging apparatus utilizing 3D printed customized mounting hardware that is tailored to the in vivo, pre-mortem systolic and diastolic geometries. Other factors affecting the accuracy of MV datasets include the overall orientation and medium in which the valve is scanned. Several scanning protocols with the valve submerged in air or liquid require the valve to be placed with the open leaflets oriented horizontally [1–4]. This places gravitational forces on the leaflets, causing unphysiological deformations that do not depict the valve in a realistic diastolic configuration of separated leaflets while the valve is open in a stress-free natural state. Positioning the valve vertically, with the PMs below the annulus, ensures that the resulting image data set reflect a much more realistically diastolic, stress-free state of the valve.

Imaging in fluid further improves upon this by affording tissues a degree of buoyancy similar to what the valve experiences in the heart. Ideally the density of imaging fluid should

✉ M.O. Jensen
mojensen@uark.edu

[1] Department of Biomedical Engineering, University of Arkansas, Fayetteville, AR, USA

[2] Departments of Radiology and Surgery, University of Arkansas for Medical Sciences, Little Rock, AR, USA

[3] Division of Neurotoxicology, National Center for Toxicological Research, US Food and Drug Administration, Jefferson, AR, USA

[4] Department of Mechanical Engineering, University of Kentucky, Lexington, KY, USA

be a close match to blood to ensure natural buoyancy forces. Additionally, it has been shown that imaging in air can lead to several undesirable effects associated with surface tension [3]. Attractive forces are exerted upon adjacent tissues by residual moisture on their surfaces; the Chordae Tendineae (CT) and leaflet edges are particularly susceptible due to their flexibility and thin nature. Valves imaged in air, unless quite dry, can experience leaflet curling and clumping of the CT. These tendencies can be eliminated by using a fluid imaging medium, which is the natural environment for the valve. Additionally, valves and other tissues will desiccate if left unsubmerged in liquid fluids, particularly in longer scans. This frequently leads to tissue shrinkage which causes movement during imaging, impairing or ruining the dataset, as well as potentially rendering the tissue unsuitable for any subsequent biomechanical testing, which is vital for important boundary conditions to computational models.

One major advantage of μCT over high field MRI is dramatically shorter scan times. MRI scan times frequently stretch to many hours, perhaps even as high as 100 h [10], depending on the size of the object and the required resolution. The maintenance of tissue integrity and stability over this timeframe can be challenging, particularly when attempting to image tissue which must maintain a constant 3D configuration throughout the scan in whichever state it is imaged in. Compared to MRI, similar resolution scans can be completed using μCT with a scan time that is significantly shorter. The use of a fluid imaging medium is however more challenging in μCT than MRI. Perfluoropolyether (PFPE) oils are commonly used with imaging with tissues in MRI. While well suited to MRI imaging, these oils are very expensive, and present several logistical challenges. As μCT primarily utilizes density to discern different materials, the relatively close match between the density of tissue and most fluids leads to a very low difference in intensity of the MV sample and the background. This can be overcome by employing contrast enhancing staining techniques such as diffusible iodine-based contrast-enhanced computed tomography (DiceCT) [11] to enhance the discerning of the MV from the background of the fluid medium.

The following is a description of a newly developed technique for obtaining high resolution datasets for the MV in the natural state within a fluid by employing DiceCT, with evaluations of several staining procedures and fluid medium options. Ultimately, this provides a more accurate representation of the MV in a stress-free configuration, which is essential for biomechanical modeling.

Methods

Hearts were obtained from approximately 180 lb. pigs from a local abattoir, and the MV was removed. Valves were prepared by trimming the PMs to approximately ¼" below the lowest CT insertion point and removing as much myocardium from around the annulus as possible. The MVs were then immediately stained using Lugol's solution (I_2KI, Lugol's solution, Sigma, L6146). Sufficient solution was used to immerse each valve and prevent the solution from becoming depleted (details below). To promote uniform iodine absorption, the solutions were agitated throughout staining. Following staining, the valves were then thoroughly rinsed in clean deionized water to fully remove any residual Lugol's solution from the surface of the tissue. The valves were kept damp and chilled until scanned. All valves were scanned within 1 h from removal of the staining solution. Prior to scanning, the MVs were mounted within a temporary imaging apparatus which suspends the valve by the PMs, ensuring that the CT remain taut. Imaging fluid (details below) is added to the apparatus immediately prior to scanning to avoid artefacts from iodine leaching into the imaging fluid.

Fluid Study

To aid in determining an ideal imaging fluid medium, several MVs were stained identically and scanned within different fluids. The fluids selected for study were deionized (DI) water, 90% ethanol, *Olea europaea* oil and glycerol. DI water and ethanol were chosen as they have been frequently employed in previous studies [11, 12]. *Olea europaea* oil and glycerol were selected to evaluate both a non-polar and substantially viscous liquid, respectively. Staining procedure parameters for all fluid study valves were 1% *w*/*V* iodine for 90 min, followed by thoroughly rinsing in clean DI water.

Staining Study

In an effort to optimize the staining procedure, several MVs were imaged within one of the imaging fluids with differing stain concentrations and times. *Olea europaea* oil was chosen as the imaging fluid for the staining study based on results discussed below. These valves form a separate set from those used in the fluid study. Iodine concentrations and stain times considered were 0.5%, 1.28%, 2.06% and 2.85% (stock solution) for 0.5 to 5.5 h in one-hour increments. Valves were dissected and stained throughout the day in which they were scanned, starting with those that were stained longest, which were the first ones scanned. The valves that were stained for shorter durations were started later in the day in order to have all valves finish the staining process shortly before they were to be scanned. This eliminates the need to store those that finish earlier if they were all started at the same time as many storage solutions can cause iodine to leach back out of the tissue.

The datasets obtained in this study are also used to evaluate the degree at which iodine potentially leaches out of the tissue

and into the background of the imaging fluid. This is done by examining the data that was not reconstructed, that is, the stack of images taken as the sample rotates on the μCT turntable prior to reconstruction into z-axis slices. The scanner is setup so that the first and last of the un-reconstructed images overlap. This is often useful in determining whether the sample moved during scanning by toggling between the images and checking for differences. Because the geometry in these images overlap, and they represent the time points at which the MV has just been immersed and when it has been immersed the longest, these images can also be used to evaluate any change in average background intensity, primarily due the leaching of iodine from the tissue. This background intensity change is evaluated close to the tissue surface as the iodine leaching is occurring at the tissue-background interface and because it is unclear whether any leached iodine will sufficiently diffuse through the fluid medium to cause a homogeneous intensity change.

A standard least squares regression analysis along with ANOVA is applied to the results from the staining study. The equation below represents the model used in the least squares analysis.

$$Y = \beta_0 + \beta_1 X_1 + \beta_2 X_2 + \beta_3 X_1 X_2 + \in$$

Where:

Y is the tissue-background contrast
X1 is the stain concentration for the solution in which the valves are submersed
X2 is the time that the mitral valves are left in the stain solution
$\in$ is the independent error term that follows a normal distribution with mean 0 and equal variance σ^2

The null hypothesis is:

- $H_0 : \beta_1 = \beta_2 = \beta_3 = 0$
- $H_A : At\ least\ one\ \beta_j \neq 0$

This test will determine whether there is a significant factor affecting contrast and which factor(s) (stain time and/or concentration) are the most likely to significantly impact the contrast of the mitral valve scan. It is assumed that a p value of 0.05 or lower is significant. Statistical analysis is conducted using JMP (SAS, Cary, NC).

Physiological Configuration

The motivation for scanning in fluid for this case study is to improve the physiological correspondence of the mitral valve, where a final, more physiologically realistic configuration of the MV was considered in which the annulus was secured in a 3D printed, physiologically contoured clamp. This dataset is intended to serve as a demonstration of the quality, physiologically realistic 3D surface model that can be generated from the above described imagery. The design and fabrication of these clamps has previously been reported [1]. The trimmed annulus (of a new valve, separate from the fluid and staining study) was stained and then sutured to one half of the clamp through integrated suture holes spaced evenly around the annulus. Once secure, the other half of the two-piece clamp was attached using plastic screws. The PMs were sutured to adjustable holders and the mounted valve was affixed to an acrylic scaffold. The PM holders maintained slight tension in the CT to prevent drooping. Staining parameters for this valve were 90 min in a 2.85% *w*/*v* iodine solution.

All valves were scanned within a Nikon X TH 225 ST (Nikon, Tokyo, Japan) μCT scanner. A 225 kV rotating source was used with a Perkin Elmer 1620 detector. The machine was thoroughly warmed up and conditioned prior to all scans. Automatic background subtraction was performed prior to each batch of scans. Scanner settings were held constant at 173 kV and 192 μA with a 0.125-in.-thick copper filter. All scans utilized the same attenuation coefficient scaling. No image averaging was performed. All samples were elevated from the metal manipulator using Styrofoam blocks to avoid scatter. Samples were rotated 360° to obtain 3141 images for each scanning session. These scans took approximately 15 min each and had an isotropic voxel resolution of 31 μm. All datasets were reconstructed using CT Agent, CT Pro 3D (Nikon) and VGStudio MAX (Volume Graphics, Heidelberg, Germany). All image edits and 3D surface model rendering were performed using ImageJ version 1.54 [13]. Image editing was performed on the physiological dataset and includes primarily operations such as masking out unwanted areas including the container and mounting features. Additionally, ring artifact corrections were applied to several scans. All scans and reconstructions were performed at the University of Arkansas MicroCT Imaging Consortium for Research and Outreach (MICRO). The scanning setup is shown in Fig. 1.

Results

Example images from the fluid study are presented in Fig. 2. Also shown are example images for scans done of an unstained valve in air, which is the most conventional arrangement, as well as an unstained valve immersed in water. Due to the very different contrasts from the previously considered cases it was not possible to maintain the same scanner settings for these two additional valves. They do nonetheless serve to illustrate that while resolving stained tissue in fluid is not, and likely will never equal that of tissue in air, it does offer a dramatic improvement over immersed, unstained tissue.

The average surface and nearby background greyscale values for the stained valves are presented in Table 1, along

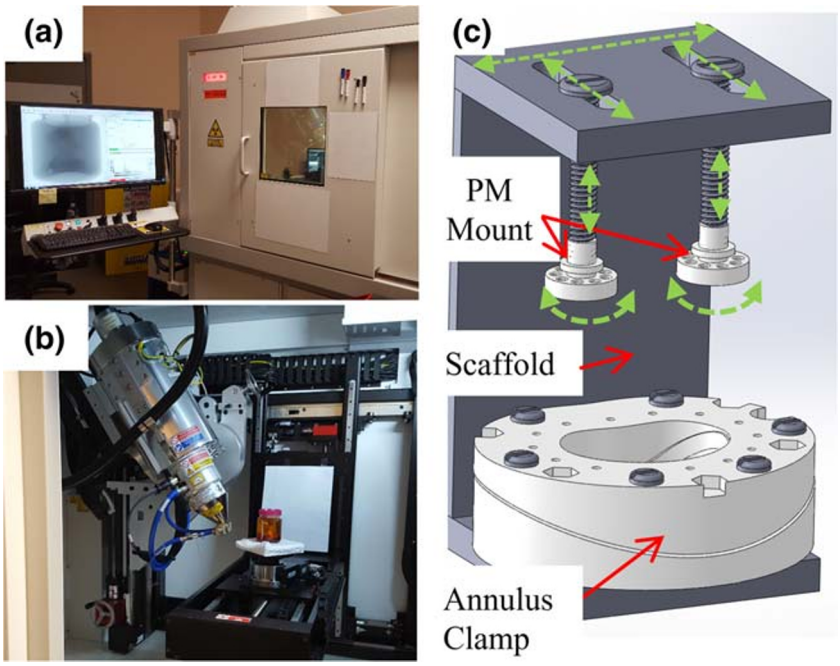

Fig. 1 μCT scanning setup showing (**a**) exterior of device with example "scouting" scan, (**b**) interior of μCT scanner with X-ray source (left) and fluid immersed valve in plastic container mounted atop Styrofoam (center) and (**c**) the valve mounting scaffold and hardware used to position the physiologically anchored valve. PM positioning degrees of freedom shown in green

with the contrast between the two, defined here as the surface average minus the background average. Surface intensities were measured using ImageJ by manually drawing regions of interest (ROI) enclosing only the thin outer layer of tissue that has been stained and finding the ROI average. Several ROIs were drawn for each image stack and the results averaged. The primary region of interest in this case study is the mitral leaflets, so stain anisotropy was not an issue as only regions showing leaflet tissue were considered for contrast measurements.

All stained valves showed significantly increased contrast when imaged in fluid compared to unstained valves, which are all but indiscernible from the background. The contrast is far greater for *Olea europaea* oil than the other fluids. Noise was quantified by measuring the standard deviation of the histogram taken over a ROI enclosing a nearly uniform region of background. All scans had a similar standard deviation with the average being approximately 1100 (of a maximum dynamic range of 65,536 for 16-bit greyscale images).

During scanning it was observed that the glycerol seemed to cause significantly greater tissue movement, requiring the sample to be rescanned several times to obtain a high-quality, movement-free dataset. This is perhaps due to the higher density, and thus inertia, of glycerol relative to the tissue. Entrained air bubbles clinging to the tissue surface due to surface tension were more difficult to remove from both the glycerol and *Olea europaea* oil samples. These bubbles, which present themselves as dark regions that typically lie directly adjacent to the tissue (Fig. 3), did not strongly affect the intensity measurements as they were few enough to easily be excluded from the regions over which intensity averages are computed.

Figure 3 shows example images taken at approximately the same location along the staining study valves. Staining parameters as well as average surface and background intensity are presented for all staining study valves in Table 2. Contrast is computed as average surface intensity minus the average background intensity. Table 2 additionally provides the change in background intensity between the initial and final un-reconstructed image. These background intensities were evaluated close to but not touching the MV annulus. Any change in near-tissue background intensity is attributed to iodine leaching from the stained tissue into the medium.

Table 3 gives the results from the statistical analysis. The table shows two values, the F-ratio and the p value. The F-ratio results from the ANOVA calculations from using multiple independent variables. The p value indicates significance from the goodness-of-fit-test, or in other words the null hypothesis. Since we have at least one p value lower than 0.05, the results from the staining study demonstrate that the null hypothesis is invalid and a factor significantly impacts the contrast. As can be seen from the table, the p values for the stain concentration and the stain time are independently lower than 0.05 which indicates a high likelihood of significance. The higher combination p value indicates no interrelated increase of contrast from these two variables. A clear representation of the model can be seen in Fig. 4.

Figure 5 is the resulting 3D rendering from a scan of the MV mounted within a physiologically shaped annulus clamp and stained with a 2.85% staining solution for 90 min. The valve is mounted in the imaging apparatus depicted in in Fig. 1. The mounting features have been removed from the images for clarity of view of the valve.

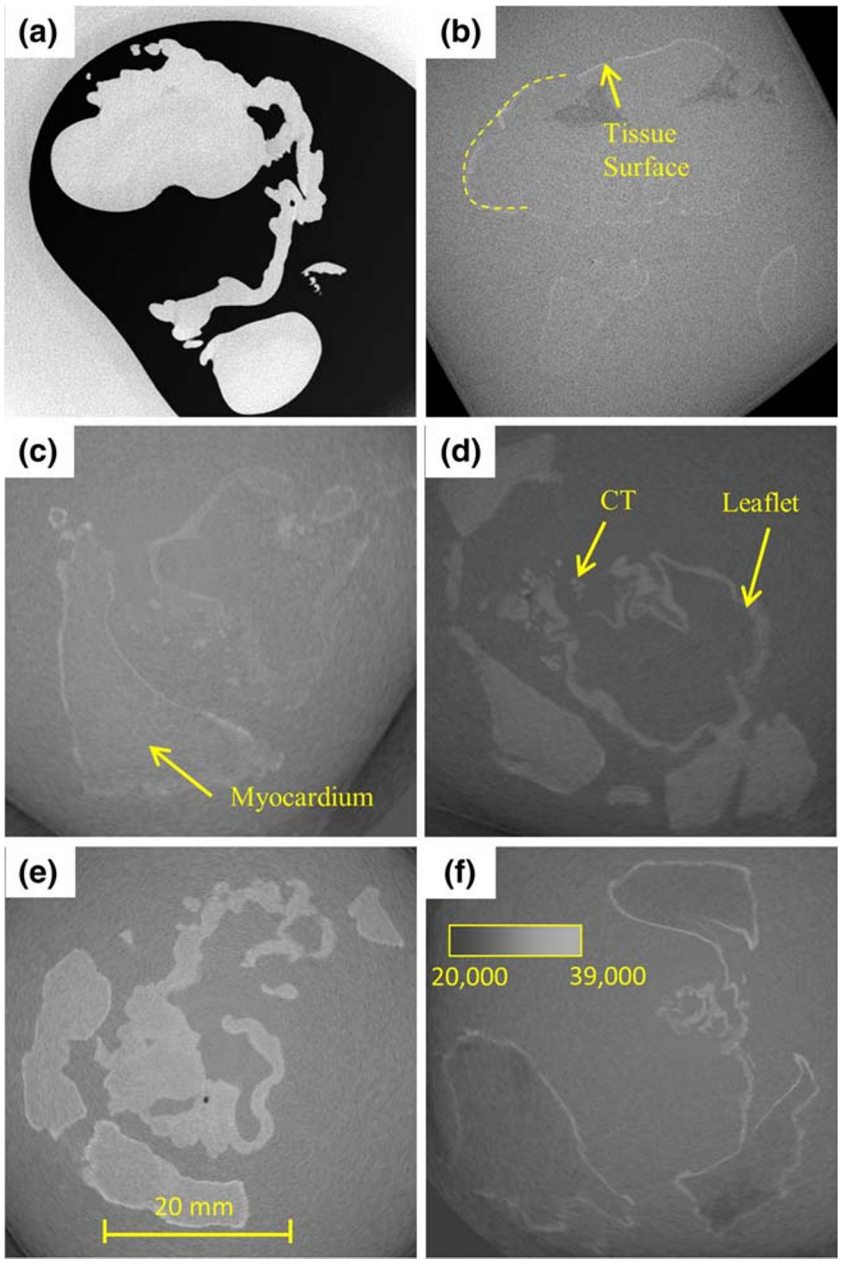

Fig. 2 Example images from fluid study. All slices intersect approximately the same anatomical structures on each valve, specifically forming a plane through the leaflets. For comparative purposes unstained valves in (**a**) air and (**b**) deionized water have been included. Stained valves were stained in 1% w/v iodine solution for 1 ½ hours and scanned in: (**c**) deionized water, (**d**) 95% ethanol, (**e**) Olea europaea oil and (**f**) glycerol

Discussion

The techniques described for using DiceCT imaging of MVs within an Olea europaea oil bath are demonstrated to produce high quality datasets that can easily be used to construct a high-resolution 3D surface model or rendering. The stained tissue contrast in Olea europaea oil was significantly better than the second-best fluid tested and a vast improvement over water. All stained valves, regardless of staining parameters of imaging medium, show improved contrast over immersed

Table 1 Average greyscale values for fluid study valves. Maximum dynamic range for 16-bit greyscale images is 65,636. Contrast is the average surface intensity minus the average background intensity

Fluid Medium	Surface Average Intensity	Background Average Intensity	Contrast
DI Water	39,310	35,379	3931
Olea europaea oil	43,134	32,832	10,301
90% Ethanol	26,573	21,821	4751
Glycerol	33,345	29,564	3781

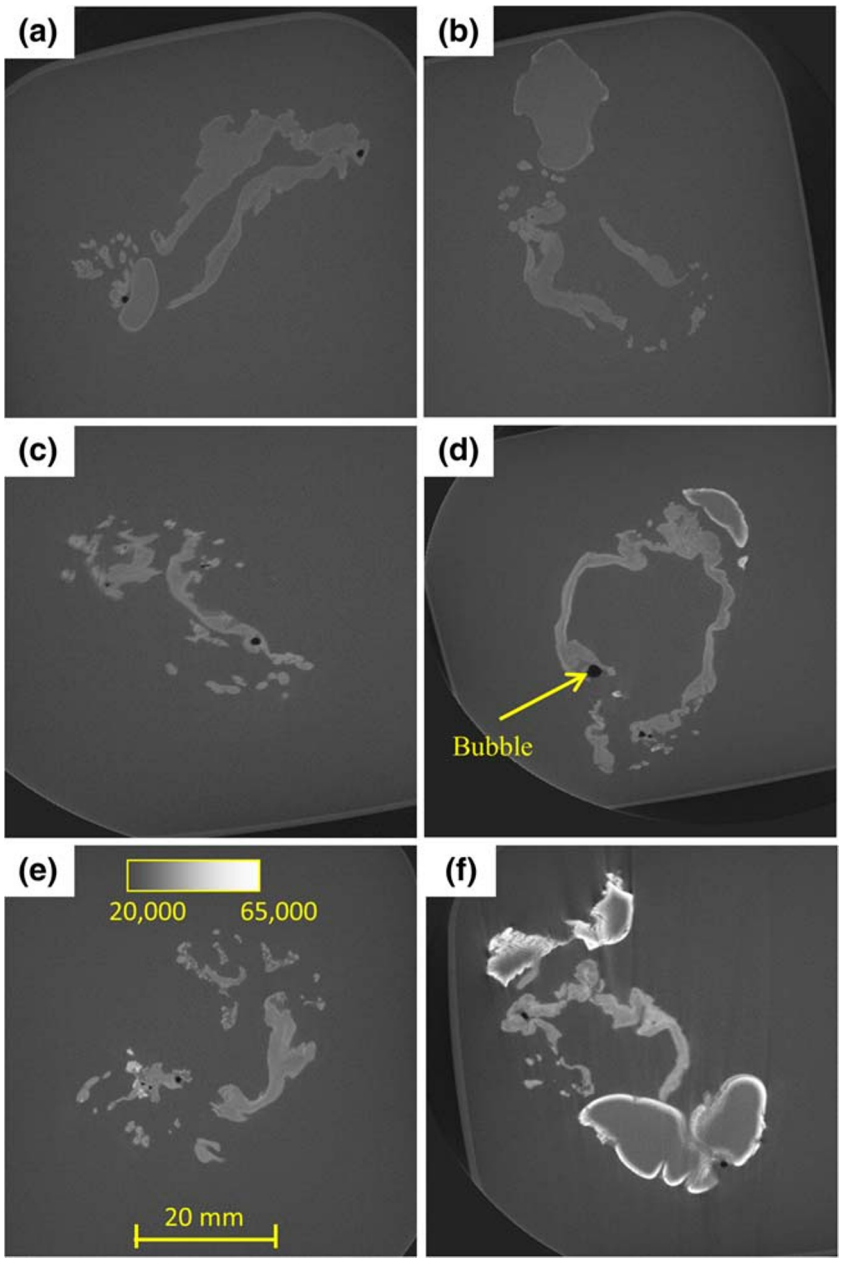

Fig. 3 Example images from staining study. All slices intersect approximately the same anatomical structures on each valve. All valves were scanned in Olea europaea oil with the following staining parameters: (**a**) 0.5 h @ 0.5% *w/v*, (**b**) 3.5 h @ 0.5% *w/v*, (**c**) 0.5 h @ 1.28% w/v, (**d**) 3.5 h @ 1.28% *w/v*, (**e**) 0.5 h @ 2.85% w/v and (**f**) 3.5 h @ 2.85%

unstained valves. Stain time and concentration appear to have a strong impact on the quality of the scan. Generally, shorter stains at a higher concentration (of those considered here) produce the best results, though there is an upper limit, as too much iodine uptake into the tissue leads to x-ray scattering which creates undesirable artifacts. An example of x-ray scattering due to excessive iodine uptake can be seen in Fig. 3(f). While such scattering artifacts are not quantified here or otherwise included in the current analysis, they should nevertheless be avoided as they can severely impair image quality. High stain concentrations coupled with high staining times also appear to lead to increased iodine leaching into the fluid medium. Adding imaging fluid immediately prior to scanning minimizes this leaching of iodine into the fluid during storage and scanning.

Ethanol is perhaps the most common medium used in conjunction with DiceCT. The results presented here show that substantially better image contrast can however be achieved by using other fluids, with Olea europaea oil being one example. DiceCT specimens have typically had their tissues previously fixed, which makes ethanol an ideal storage and imaging medium. For fresh tissues, particularly if subsequent mechanical studies are intended, the use of ethanol can be further detrimental as it displaces water from the tissues. This alters the tissue's material behavior, hampering the correlation between geometric and mechanical measurements. This presents

Table 2 Staining parameters and average greyscale intensity values (out of a maximum 65,636) for staining study in Olea europaea oil. Contrast is the average surface intensity minus the average background intensity. Change in background intensity is computed as the difference in average background intensity between the first and final of the unreconstructed, rotating images

Concentration (% w/v)	Time (hr:min)	Surface Average Intensity	Background Average Intensity	Contrast	Change in Background Intensity
2.85	0:30	33,853	21,222	12,631	140
2.06	0:30	29,076	21,002	8075	251
1.28	0:37	28,593	20,823	7770	296
0.5	0:37	25,386	20,695	4692	298
2.85	1:35	35,791	21,154	14,637	305
2.06	1:35	29,704	20,914	8789	330
1.28	1:30	28,214	20,297	7917	497
0.5	1:30	25,641	20,839	4802	426
2.85	2:15	36,700	21,565	15,135	351
2.06	2:15	31,229	20,682	10,548	247
1.28	2:40	29,489	20,796	8693	296
0.5	2:40	25,442	20,822	4621	364
2.85	3:30	39,087	20,743	18,343	372
2.06	3:30	32,138	20,884	11,254	347
1.28	3:40	31,169	21,157	10,012	323
0.5	3:40	26,098	20,675	5423	373
2.85	4:46	38,999	20,882	18,117	344
2.06	4:41	33,211	21,457	11,754	303
1.28	4:40	32,380	20,949	11,431	285
0.5	4:40	25,915	20,831	5084	381
2.85	5:25	41,625	22,036	19,589	341
2.06	5:25	33,233	20,833	12,400	339
1.28	5:30	32,726	20,522	12,204	336
0.5	5:30	26,484	20,743	5740	330

a serious issue as the imagery obtained in this study is primarily intended for use in computational simulations, input which requires such a direct correlation. Olea europaea oil on the other hand is inert and can be easily washed from the tissue surface. The impact of staining in Lugol's solution upon tissue mechanical behavior is not clear and is beyond the current scope of this study. Throughout the work presented here however, no significant alteration to the tissue's mechanical behavior was observed qualitatively, certainly not to the extent that would be typical of conventional fixation.

Olea europaea oil was selected because it is non-polar and is also in literature shown it to have a significantly lower x-ray mass attenuation coefficient than water, a reduction of approximately 25% [14]. A fluid with a lower attenuation coefficient more easily allows x-rays to travel through to the immersed

Table 3 Results from staining study statistical analysis

Statistical Significances		
Source	F-ratio	p value
Stain concentration	72.0954	<0.0001
Stain time	11.6546	0.0028
Stain concentration*Stain time	0.4195	0.5246

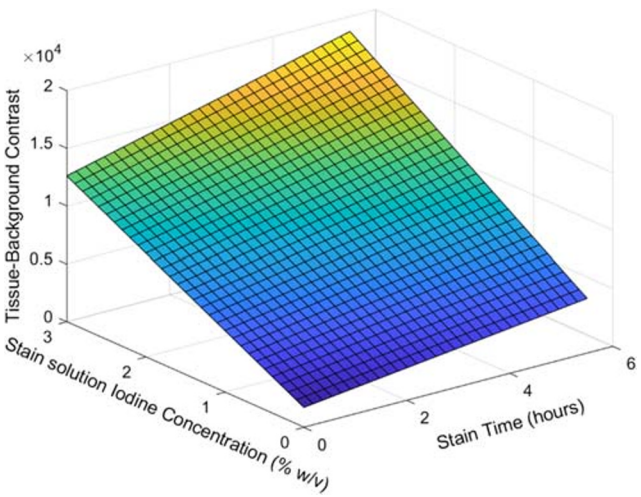

Fig. 4 A graphical model of the correlation from Time stained and Percentage of stain. The equation is $Y = 785.68 + 4188.70 * X_1 + 858.80 * X_2 + 185.82 * (X_1 - 1.67) * (X_2 - 3.05)$ where X_1 is the Stain concentration and X_2 is the stain time in hours

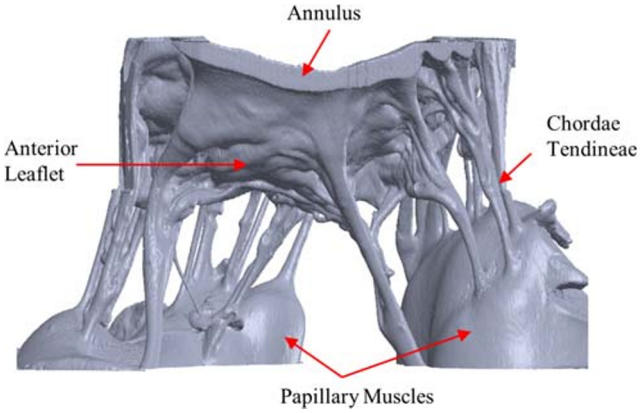

Fig. 5 Valve mounted using physiological annulus clamp. Mounting features are not rendered for clarity, and data cutoffs at the periphery of the image are chosen to focus on the rendering of the central aspects of the valve

sample and thus leads to higher quality imagery. Determining the mass attenuation coefficient for a fluid is however nontrivial as it depends upon atomic mass and total photon cross sectional area, and is further a function of x-ray energy [15]. While the calculation is certainly possible it becomes increasingly difficult to identify an ideal fluid from an arbitrarily long list. For the purposes of immersing biological samples, an empirical approach to selecting imaging mediums may prove most fruitful.

While not quantitatively measured, it is observed that the stained tissue depth increases for longer staining durations. This agrees with the diffusion-based uptake model commonly applied. As this study is concerned only with surface geometry rather than internal structure, maximum contrast between the MV surface and the background fluid is the primary aim. For this same reason, stain anisotropy is not a concern in this study. The mitral valve is a complex structure that is composed of several different tissues. The primary motivation for the development of DiceCT was the discernment of different soft tissues from one another, so it therefore should be of no surprise that the scans presented show different structures absorbing stain at different rates. For the scans presented, the most weakly stained portions still possess sufficient contrast with the background as to facilitate high fidelity 3D reconstruction as demonstrated in Fig. 5.

The creation of MV computational models requires high-resolution geometry data as an input. Such models promise the ability to simulate the performance and effects of medical devices and procedures, as well as validating the material properties of the MV tissues. This ability would eventually improve patient outcome by permitting the testing and evaluation of various surgical options in silico, particularly when generated with patient specific geometry from clinical imaging modalities. It is clear that these modalities are not currently providing the same resolution and quality as the experimental modality used here. However, it is important to first focus on the development of material properties and validating the models to combine clinical imaging with computational biomechanics. That is the exact premise of future studies that will extend from the results presented in this work.

Limitations and Future Directions

The effects of iodine leaching from the tissue into imaging medium were measured in this study and found to not be significant relative to the tissue-background contrast, particularly for the relatively short scan times considered. A more thorough investigation into iodine leaching would be of interest when truly optimizing a staining protocol or when longer scan times are required.

Additionally, the use of contrast enhancing stains increases the intensity of tissues to near the same values of many 3D printed plastics. This makes the removal of valve mounting elements, such as the two-piece clamp employed in this study, more challenging as they inherently are in contact with the tissues, complicating intensity-based separation techniques. An algorithm is currently being developed to automatically remove mounting hardware from z-axis slice images by geometric means rather than intensity. As these pieces of hardware are 3D printed, their precise geometry and orientation is known, allowing for the creation of masks corresponding to the relevant slices in which they appear.

Conclusion

To ensure reliable results from computational simulations of heart valves, high quality imagery is required, particularly in the stress-free state. A new imaging protocol for using μCT imaging of the mitral valve in liquid has been demonstrated. This imagery coupled with measurements of loading in a valve-specific spatial configuration will permit direct validation of computational models in future studies.

Acknowledgements The authors wish to thank Cockrum Taxidermy in Rudy, Arkansas for donating the porcine hearts used in this study. Additionally, the authors wish to thank the staff of the University of Arkansas MICRO group, in particular Manon Wilson.

Funding Research reported in this publication was supported by the National Heart, Lung, And Blood Institute of the National Institutes of Health under Award Number R15 HL145585-01. The content is solely the responsibility of the authors and does not necessarily represent the official views of the National Institutes of Health. Additional support was provided through NSF Grant Number NSF BCS-1725925 for the University of Arkansas MicroCT Imaging Consortium for Research and Outreach and National Center for Toxicological Research Protocol Number Z999928. The information in these materials is not a formal

dissemination of information by the FDA and does not represent agency or policy.

Compliance with Ethical Standards

Conflict of Interest The authors declare that they have no conflict of interest. The information in these materials is not a formal dissemination of information by the FDA and does not represent agency or policy.

References

1. Stephens SE, Liachenko S, Ingels NB, Wenk JF, Jensen MO (2017) High resolution imaging of the mitral valve in the natural state with 7 tesla MRI. PLoS One 12(8):e0184042. https://doi.org/10.1371/journal.pone.0184042
2. Rabbah JP, Saikrishnan N, Yoganathan AP (2013) A novel left heart simulator for the multi-modality characterization of native mitral valve geometry and fluid mechanics. Ann Biomed Eng 41(2):305–315. https://doi.org/10.1007/s10439-012-0651-z
3. Toma M, Bloodworth CH, Einstein DR, Pierce EL, Cochran RP, Yoganathan AP, Kunzelman KS (2016) High-resolution subject-specific mitral valve imaging and modeling: experimental and computational methods. Biomech Model Mechanobiol 15(6):1619–1630. https://doi.org/10.1007/s10237-016-0786-1
4. Bloodworth CH, Pierce EL, Easley TF, Drach A, Khalighi AH, Toma M, Jensen MO, Sacks MS, Yoganathan AP (2017) Ex vivo methods for informing computational models of the mitral valve. Ann Biomed Eng 45(2):496–507. https://doi.org/10.1007/s10439-016-1734-z
5. Jensen MO, Siefert A, Yoganathan AP (2018) Measurement technologies for heart valve function. In: Sacks M, Liao J (eds) Advances in heart valve biomechanics: Valvular physiology, mechanobiology and bioengineering, vol 1. Eds. Sacks M, Liao J, Springer Nature. https://doi.org/10.1007/978-3-030-01993-8
6. Jimenez JH, Liou SW, Padala M, He Z, Sacks M, Gorman RC, Gorman JH 3rd, Yoganathan AP (2007) A saddle-shaped annulus reduces systolic strain on the central region of the mitral valve anterior leaflet. J Thorac Cardiovasc Surg 134(6):1562–1568. https://doi.org/10.1016/j.jtcvs.2007.08.037
7. Jensen MO, Jensen H, Levine RA, Yoganathan AP, Andersen NT, Nygaard H, Hasenkam JM, Nielsen SL (2011) Saddle-shaped mitral valve annuloplasty rings improve leaflet coaptation geometry. J Thorac Cardiovasc Surg 142(3):697–703. https://doi.org/10.1016/j.jtcvs.2011.01.022
8. Jimenez JH, Soerensen DD, He Z, Ritchie J, Yoganathan AP (2005) Effects of papillary muscle position on chordal force distribution: an in-vitro study. J Heart Valve Dis 14(3):295–302
9. Cochran RP, Kunzelman KS (1998) Effect of papillary muscle position on mitral valve function: relationship to homografts. Ann Thorac Surg 66(6 Suppl):S155–S161. https://doi.org/10.1016/s0003-4975(98)01100-x
10. Edlow BL, Mareyam A, Horn A, Polimeni JR, Witzel T, Tisdall MD, Augustinack JC, Stockmann JP, Diamond BR, Stevens A, Tirrell LS, Folkerth RD, Wald LL, Fischl B, van der Kouwe A (2019) 7 tesla MRI of the ex vivo human brain at 100 micron resolution. Sci Data 6(1):244. https://doi.org/10.1038/s41597-019-0254-8
11. Gignac PM, Kley NJ, Clarke JA, Colbert MW, Morhardt AC, Cerio D, Cost IN, Cox PG, Daza JD, Early CM, Echols MS, Henkelman RM, Herdina AN, Holliday CM, Li Z, Mahlow K, Merchant S, Muller J, Orsbon CP, Paluh DJ, Thies ML, Tsai HP, Witmer LM (2016) Diffusible iodine-based contrast-enhanced computed tomography (diceCT): an emerging tool for rapid, high-resolution, 3-D imaging of metazoan soft tissues. J Anat 228(6):889–909. https://doi.org/10.1111/joa.12449
12. Metscher BD (2009) MicroCT for comparative morphology: simple staining methods allow high-contrast 3D imaging of diverse non-mineralized animal tissues. BMC Physiol 9:11. https://doi.org/10.1186/1472-6793-9-11
13. Rueden CT, Schindelin J, Hiner MC, DeZonia BE, Walter AE, Arena ET, Eliceiri KW (2017) ImageJ2: ImageJ for the next generation of scientific image data. BMC Bioinformatics 18(1):529. https://doi.org/10.1186/s12859-017-1934-z
14. Shastry A, Palacio-Mancheno PE, Braeckman K, Vanheule S, Josipovic I, Van Assche F, Robles E, Cnudde V, Van Hoorebeke L, Boone MN (2018) In-situ high resolution dynamic X-ray microtomographic imaging of olive oil removal in kitchen sponges by squeezing and rinsing. Materials (Basel) 11(8). https://doi.org/10.3390/ma11081482
15. Hubbell JH, Seltzer SM (2004) X-Ray Mass Attenuation Coefficients. https://doi.org/10.18434/T4D01F

Publisher's Note Springer Nature remains neutral with regard to jurisdictional claims in published maps and institutional affiliations.